POSSIBLE DETECTION OF SURFACE WATER ICE IN THE LUNAR POLAR REGIONS USING DATA FROM THE MOON MINERALOGY MAPPER (M^3).

S. Li[1,2], R. E. Milliken[1], P. G. Lucey[2], and E. Fisher[1], [1]Brown University, Providence, RI, 02912, [2]University of Hawaii at Manoa, Honolulu, HI 96822, shuai_li@brown.edu

Introduction: The low temperatures of regions of permanent shadow may allow cold trapping of volatiles that propagate through the lunar exosphere [1], and such deposits may preserve a record of the composition and evolution of volatiles in the inner solar system. Knowing the distribution of water ice on the Moon is critical for understanding its origin, stability, processes of deposition, and its viability for *in situ* resource utilization.

Measurements of epithermal neutrons indicate a hydrogen abundance in the upper 10s cm of lunar regolith with a water-equivalent content ranging from ~1 to >10% if all observed hydrogen were bounded with oxygen [2,3]. About 5% water (OH&H_2O) was observed during the LCROSS cratering experiment at the crater Cabeus [4]. Earth-based S band radar observations of regions near the lunar south pole suggested only 1-2% rather than massive water ice [5], whereas recent bistatic radar measurements of the LCROSS target crater Cabeus suggest the presence of small amounts of buried water ice [6]. Finally, the presence of surface water ice has been reported by Hayne, et al. [7] based on a UV band ratio sensitive to the presence of H_2O.

This study reports the detection of water ice bands exploiting indirect lighting in regions of permanent shadow using reflectance data acquired by the Moon Mineralogy Mapper (M^3) onboard the *Chandrayaan* 1 mission. The presence of absorption features of pure water ice centered at around 1.2 μm, 1.5 μm, and 2.0 μm [8] were used as criteria for identifying water ice with M^3 data. A search for spectral bands near 3μm of M^3 data were not included due to their low signal to noise ratio (SNR) [9]. We support these measurements with the bolometric temperature measured by the Diviner radiometer, reflectance measured by the Lunar Orbiter Laser Altimeter (LOLA), and circular polarization ratio (CPR) measured by Mini-RF onboard the LRO mission.

Methods: We obtained all M^3 images acquired during the optical period 2c (OP2C) and mosaicked them from 75-90° N/S using a stereographic projection. Only data between 1 μm and 2.4 μm (band 22 – 71 of M^3 data) were applied in this study considering their higher SNR relative to longer wavelengths [9]. Given that spectra for most of M^3 pixels at our study regions are noisy because they are not in direct sunlight, but instead illuminated only by light scattered from nearby crater walls and other topographic highs, we performed a smoothing function (cubic spline) [10] on all spectra. A threshold was set for the smoothing function to avoid smearing weak absorptions. Detection of ice was only performed on pixels with median M^3 reflectance greater than 0.01 to ensure the signal is sufficiently high for detection.

The positions of absorption shoulders and centers of pure water ice reported by Clark [8] were applied as criteria for identifying ice in the lunar polar regions (Table 1). If the left and right shoulders and center of an absorption were within appropriate ranges (Table1), then a feature was marked as a potential ice absorption. Pixels were marked as ice-bearing if their spectra exhibited three such absorptions centered near 1.2 μm, 1.5 μm, and 2.0 μm, matching all conditions in Table 1. Spectral angles between the spectra of potential ice deposits and the spectrum of pure ice shown in Fig. 2 were also calculated, and a spectral angle less than 30° was applied to further constrain the possible ice deposits.

We examined the Diviner maximum bolometric temperature, LOLA albedo, and Mini-RF CPR data for comparisons with M^3 observations. The maximum temperature values were applied for overlapping measurements during mosaicking. The Mini-RF CPR data were CDR mosaics downloaded from the PDS and LOLA albedo data were from Lucey, et al. [11].

Table 1. Characteristics of ice absorptions at the region of 1.0-2.4μm [8]

Absorption (μm)	Shoulder (μm)		Center (μm)	
	Min	Max	Min	Max
1.2	1.130	1.350	1.242	1.323
1.5	1.420	1.740	1.503	1.659
2.0	1.820	2.200	1.945	2.056

Results and Discussion: A number of M^3 pixels consistent with the presence of water ice were identified within 15° of the poles. However, most of the detections were located within 5° of the poles, which is shown in Fig. 1. The maximum Diviner temperature, LOLA albedo, and Mini-RF CPR data in such regions are also shown in Fig. 1.

Our results show that the southern polar region exhibits more potential ice-bearing M^3 pixels than the north. All detections were single pixels (~1x1 km after projection). Potential ice deposits at high southern latitudes occur at regions with temperature less than 110 K (Fig. 1), though maximum temperatures at other positive M^3 pixels correspond to higher values (110-180K) where water ice is likely not stable. Potential ice deposits are mostly associated with LOLA high albedo pixels near both poles, but not all LOLA high albedo regions show the presence of ice (Fig. 1). The spatial coherence of ice with LOLA high albedo is more promising in the southern polar region than the north. , our results do not show clear spatial correlation with high CPR regions observed by Mini-RF.

Examples of M^3 spectra of possible ice deposits are shown in Fig. 2, and simulation of these spectra using Hapke radiative transfer modeling suggests >20% ice content for the spectrum at the rim of crater Faustini (Fig. 2) and >10% of ice for the spectrum at the crater Peary. An example spectrum that did not pass our criteria but that shows other spectral features is presented in Fig. 2. However, we continue to investigate the possibility that the positive output of our model was caused by random noise.

The low Diviner maximum temperature and high LOLA albedo at potential ice spots seen in some M^3 pixels are consistent with the presence of ice, but similar absorptions for warmer locations indicates that such ice is not stable and is transient or that these are false detections (due to low SNR). The LOLA high albedo values could also exist at regions with steep slope, low maturity, and fine particles [11], which explains why not all LOLA high albedo regions exhibit potential ice in M^3 data. Radar observations can be complicated by surface/sub-surface roughness [12], and thin ice deposits may not allow sufficient radar scattering for their detection [5]. Thus, the absence of spatial correlation between ice deposits and Mini-RF high CPRs may suggest that the ice deposits are thin. However, detection of ice using M^3 data is constrained by the low SNR and the availability of such data. More ice could exist in the lunar polar regions than reported in this study, and additional high-resolution and high SNR spectral measurements of this kind are warranted to confirm these potential ice deposits and to fully assess the distribution of water ice at the optical surface of the Moon.

References: [1] Watson, K. *et al.* (1961). *JGR*, **66**. [2] Feldman, W. C. *et al.* (1998). *Science*, **281**. [3] Mitrofanov, I. *et al.* (2010). *Science*, **330**. [4] Schultz, P. H. *et al.* (2010). *Science*, **330**. [5] Campbell, D. B. *et al.* (2006). *Nature*, **443**. [6] Patterson, G. *et al.* (2016) *LPSC*. [7] Hayne, P. O. *et al.* (2015). *ICARUS*, **255**. [8] Clark, R. N. (1981). *JGR*, **86**. [9] Green, R. *et al.* (2011). *JGR*, **116**. [10] De Boor, C. (1978). *Math. of Comp.* [11] Lucey, P. *et al.* (Under review). *ICARUS.* [12] Spudis, P. D. *et al.* (2013). *JGR*, **118**.

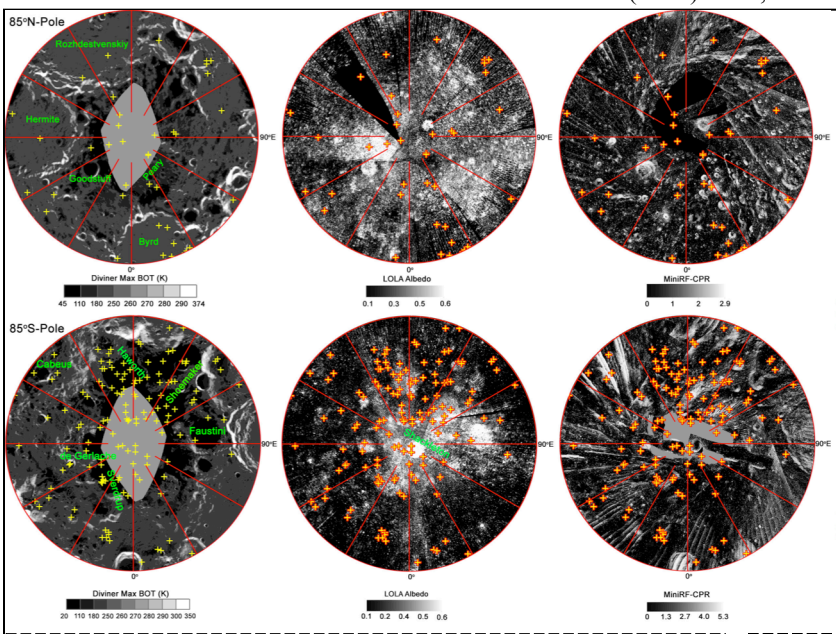

Fig. 1. Possible water ice deposits (red '+') overlain on the Diviner maximum temperature (left column), LOLA albedo (middle column), and Mini-RF CPR (right column) data in the lunar polar regions from 85° N/S to poles.

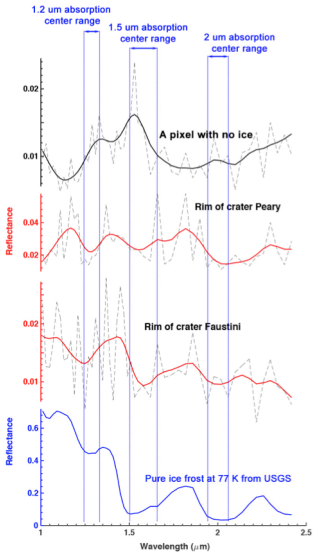

Fig. 2. Examples of M^3 spectra (dash line: original, solid line: smoothed) at locations with and without ice compared with spectra of ice.